



High frequency studies on dielectric, impedance and Nyquist properties of $\text{BaTiO}_3\text{-Li}_{0.5}\text{Fe}_{2.5}\text{O}_4$ composite ceramics substituted with Sm and Nb for microwave device applications

Ganapathi Rao Gajula¹ · K. N. Chidambara Kumar¹ · Lakshmi Rekha Buddiga² · Nirupama Vattikunta¹

Received: 3 December 2018 / Accepted: 2 January 2019 / Published online: 5 January 2019
© Springer Science+Business Media, LLC, part of Springer Nature 2019

Abstract

The $\text{BaTiO}_3\text{-Li}_{0.5}\text{Fe}_{2.5}\text{O}_4$ composite ceramics doped with Sm and Nb having chemical formulae $(90)\text{BaTi}_{(1-2x)}\text{Nb}_x\text{Sm}_x\text{O}_3+(10)\text{Li}_{0.5}\text{Fe}_{2.5}\text{O}_4$ ($x=0, 0.05$ and 0.1) were prepared using solid state reaction technique. The structural, qualitative structural information regarding functional groups, dielectric, Nyquist plots, the variation of impedance with frequency (1–10 MHz) at different temperatures, the variation of dielectric properties, A.C. conductivity and impedance with frequency between 1 MHz and 3.2 GHz at 30 °C of composites are investigated. The X-Ray diffraction peaks indicate the formation of tetragonal structure of all composites with a small amount of ferrite phase. From fourier transform infrared spectroscopy (FTIR) measurements, the presence of function groups have been identified. The dielectric studies reveal the higher value of the dielectric constant of all composites at low frequency regime due to an interfacial polarization. The dielectric constant of BTNS0.1 is higher than BTLF, BTNS0.05 which shows dispersion at low frequency region. The dielectric loss of BTLF decreases in the frequency region 80MHz–1.10 GHz. The impedance (Z') of all composites decreases with an increase in the frequency and temperature. The impedance studies show the complex behaviour of all the composites which indicates the enhancement of AC conductivity of material at higher frequencies beyond 3 GHz. The conductivity studies of composites show dispersion characteristics among the samples and the conductivity of composites is enhanced by incorporation of Nb, Sm in BTLF composites. The radii of all semi circles decrease with increase in temperature which represents conductivity of composites increases with increase in temperature.

1 Introduction

The composite ceramic material possessing high dielectric constant has technological application in modern electronic devices as actuators, capacitors, memory devices, sensors, power transmission devices, high energy storage devices [1]. The high dielectric constant materials in dielectric relaxation region have appreciable awareness in modern days [2]. The ABO_3 perovskite structure ferroelectric materials have been studied on account of their outstanding to their physical properties and these materials possess huge applications in functional technologies like actuators, transducers, sensors,

memories (FeRAM), capacitors, microwave devices, micro electromechanical systems, energy harvesting and more recently in optoelectronic devices [3–5]. The materials having ABO_3 perovskite structure have earned wider attraction because of their piezoelectric, dielectric, ferroelectric and pyroelectric properties [6, 7]. The ferroelectric materials having relaxor behavior exhibit a high frequency dispersion of dielectric permittivity [8]. BaTiO_3 is a class of ABO_3 perovskite structure. The BaTiO_3 is perovskite tetragonal structure is good ferroelectric material which has been used in variety of applications in microwave filters, resonators, mobile-communication technology and play key role in microwave devices [9, 10].

A different type of wide substitutions are possible at Ba^{2+} on A sites or Ti^{4+} on B sites independently or simultaneously in perovskite structure to alter the microstructure, dielectric and ferroelectric properties of BaTiO_3 [11]. In BaTiO_3 , when Mg^{2+} , Dy^{3+} , Tb^{3+} , Eu^{3+} , Nd^{3+} , Gd^{3+} , Yb^{3+} , Sm^{3+} , Er^{3+} , Ho^{3+} , Sb^{3+} , Sc^{3+} , La^{3+} , Nb^{5+} , Bi^{3+} are substituted in place of Ba^{2+} or Ti^{4+} , then charge imbalance takes place and vacancies are

✉ Ganapathi Rao Gajula
ganapathi.gajula@gmail.com

¹ Department of Physics, BS&H, Sree Vidyanikethan Engineering College, Tirupati, A.P 517102, India

² Department of Chemistry, Andhra University, Visakhapatnam, A.P 530 003, India

created on A sites or B sites or generation of holes in order to maintain neutral electrical charge [12–18].

The individual high conducting grains are separated by either air gaps or low-conducting layers in inhomogeneous dielectric materials which is exhibited by ferrites. One such class of ferrite is lithium ferrite widely used in potential microwave applications such as isolators, circulators and phase shifters, due to high resistivity, low eddy current losses and convincingly low costs. Moreover, many research groups have been focussed on the lithium ferrites which have fascinated appreciable interest [19]. The ferrite possesses huge electrical properties which depend on various factors like method of preparation, grain size, chemical composition, sintering temperature and atmosphere [20, 21]. The important class of spinel ferrite is lithium ferrite (LF) used in high frequency devices due to high resistivity, mechanical hardness, square loop properties and Curie temperature [22]. Development of the composite materials for high frequency applications requires rigorous understanding of the materials behavior at the frequencies of interest. On account of the structural, dielectric, electrical, thermal, optical and mechanical properties of dielectric ceramics, they yield wide attraction. These properties of dielectric ceramics make them find a room in huge applications like military electronics, communication systems, power transmission and distribution system, automation, in personal computers as well as in microwave components like dielectric resonators, microwave oscillators, antennas etc. [23, 24]. These remarkable properties are currently being used to develop frequency tunable devices in the GHz frequency range [25] and many of the research groups have been reported in the GHz frequency region [26–28]. The structural, morphological, magnetic (M-H, M-T), ferroelectric properties, the variation of dielectric properties with temperature and Magneto-electric voltage coefficient of Sm and Nb substituted $\text{BaTiO}_3\text{-Li}_{0.5}\text{Fe}_{2.5}\text{O}_4$ composites exhibited simultaneously considered as multiferroics have been reported previously [29].

In this paper we study the dielectric, impedance, Nyquist plots with frequency at different temperatures, dielectric, impedance A.C. conductivity of Sm, Nb doped $\text{BaTiO}_3\text{-Li}_{0.5}\text{Fe}_{2.5}\text{O}_4$ composite ceramics with high frequency region (1 MHz–3.2 GHz) at 30 °C has been present. We have prepared three samples ((90) $\text{BaTi}_{(1-2x)}\text{Nb}_x\text{Sm}_x\text{O}_3$ +(10) $\text{Li}_{0.5}\text{Fe}_{2.5}\text{O}_4$ ($x=0, 0.05$ and 0.1)) and labelled (90) BaTiO_3 + (10) $\text{Li}_{0.5}\text{Fe}_{2.5}\text{O}_4$, (90) $\text{BaTi}_{0.9}\text{Nb}_{0.05}\text{Sm}_{0.05}\text{O}_3$ + (10) $\text{Li}_{0.5}\text{Fe}_{2.5}\text{O}_4$ and (90) $\text{BaTi}_{0.8}\text{Nb}_{0.1}\text{Sm}_{0.1}\text{O}_3$ +(10) $\text{Li}_{0.5}\text{Fe}_{2.5}\text{O}_4$ as BTLF, BTNS0.05 and BTNS0.1 respectively.

2 Synthesis and characterizations

The Sm and Nb substituted $\text{BaTiO}_3\text{-Li}_{0.5}\text{Fe}_{2.5}\text{O}_4$ composites have been prepared using solid state reaction route. BaCO_3 (98%) (Merck), TiO_2 (99.5%), Li_2CO_3 (99%), Fe_2O_3 (98%)

(Loba Chemie), Nb_2O_5 (99.9%) (Titan biotech Ltd.), Sm_2O_3 (99.9%) (Loba Chemie) are used for preparing the composites. All the samples are weighed at an appropriate molar proportion. All the precursor of each sample are mixed in an agate motor. After 10 h of grinding, we obtain a homogeneous mixing and distribution of the ingredients. Using furnace, all the grinded samples are calcinated at 900 °C temperature for 3 h. The procedure of calcination is applying using furnace which gives heating for the samples to obtain homogeneous churn powder. These calcinated sample powders are again grinded for few hours to become fine powder. The polyvinyl alcohol is dissolved in distilled water and is heated at 80 °C, until gel is formed which acts as a binder. The gel (binder) is added to the calcinated powder and grinded well until a fine powder is obtained. The fine powder is placed into die set and pressure is applied using a hydraulic press for 3 min to form pellets. The obtained pellets are sintered for 3 h at 1150 °C. The sintered pellets and sintered powders are used for different characterizations. The structural studies were carried out with the wavelength (λ) of the X ray source of radiation is 1.5406 in the 2θ range 20–80° with step size 0.02° using Bruker D8 Advance X-ray diffractometer, The functional groups of composite samples are measured in the wave-number range (in the Mid-IR) 4000–400 cm^{-1} at room temperature (~27 °C) using fourier transform infrared spectroscopy (FTIR), Bruker, Germany, Model Vertex 70. The dielectric properties were carried out using broadband dielectric spectrometer (Wayne Kerr Electronics Pvt. Ltd., Model: 1J43100). The dielectric properties, impedance, A.C. Conductivity over High frequencies from 1 MHz–3.2 GHz at 30 °C are measured using Agilent Technologies.

3 Results and discussions

3.1 X-Ray diffraction

The X-ray diffraction pattern of BTLF, BTNS0.05 and BTNS0.1 recorded in the range 20–80° are shown in Fig. 1. The diffraction peaks of composites BTLF, BTNS0.05 and BTNS0.1 have been indexed using JCPDS card number 79-2263. We see from Fig. 1 that the diffraction peaks at 30.48°, 34.25°, 40.58° and 63.31° having indices (220), (310), (400) and (440) respectively and indexed using JCPDS no. 89-7832 & 88-06711 strongly confirms the incorporation of LF in the BTLF composite. The diffraction peaks of BTLF, BTNS0.05 and BTNS0.1 composites reveal the tetragonal structure with the presence of a small ferrite phase. The ferrite peaks of BTLF composite decreases upon doping with Nb and Sm. The diffraction peaks of BTNS0.05 and BTNS0.1 have shifted towards higher diffraction angle after doping Nb and Sm in BTLF, which again confirms

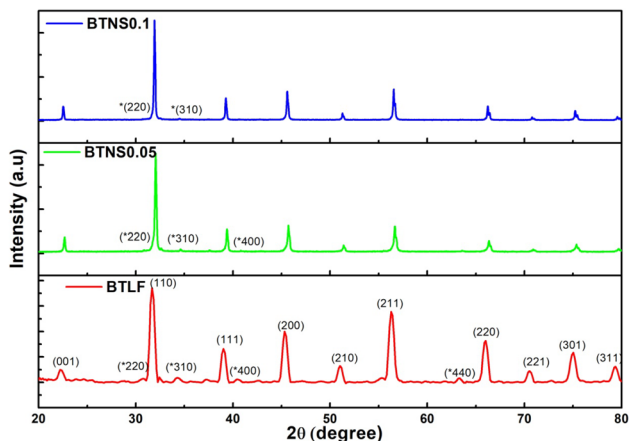


Fig. 1 X-ray diffraction pattern of BTLF, BTNS0.05 and BTNS0.1

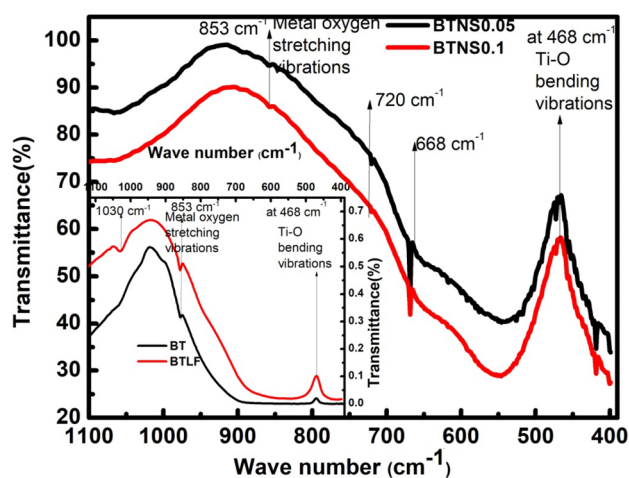


Fig. 2 FTIR spectra of BTNS0.05, BTNS0.1. Inset shows FTIR spectra of the BT, BTLF

the incorporation Nb and Sm in BTLF. Further there is no change in the structural change of BTLF composite after doping it with Nb and Sm.

3.2 Fourier transform infrared spectroscopy (FTIR)

The fourier transform infrared spectra of BTNS0.05, BTNS0.1 recorded in the wave number range 4000–400 cm^{-1} , but the bands are observed in the wave number range 1100–400 is shown in Fig. 2. The FTIR spectra of BT and BTLF are shown in the inset of Fig. 2. We see from Fig. 2, the presence of strong absorption bands at 468 cm^{-1} and 853 cm^{-1} confirms the perovskite structure of the composites. In addition to these peaks there is more peak was observed at 418 cm^{-1} , 668 cm^{-1} , 720 cm^{-1} and 1030 cm^{-1} . The bands due to bending vibrations are observed in the wavelength range 400–600 cm^{-1} and 865–950 cm^{-1} are

assigned to tetrahedral Ti–O sites and octahedral sites. The bands due to stretching vibrations are observed in the wavelength range 610–860 cm^{-1} . The difference in band positions are appeared caused by different lengths, strengths, and effective mass of the metal oxygen bonds in A and B sites of the cubic spinel, Ti, Sm, Nb in B sites of the tetragonal structure [30–32]. The presence of bands at 1030 cm^{-1} in BTLF is assigned to the stretching vibrations of the Li–O and Fe–O due to LF doped in BT. The peak at 468 cm^{-1} is allocated to the bending vibrations of the Ti–O or Nb–O or Sm–O bond in the tetragonal site and the peak at 853 cm^{-1} is allocated to control of metal oxygen stretching vibrations appearing from tetrahedral sites and oxygen complexes. Further peaks related to the presence of moisture are not observed in the FTIR spectrum. The peaks observed at 418 cm^{-1} , 668 cm^{-1} and 720 cm^{-1} are due to Sm, Nb substituted in BTLF. The peak 668 cm^{-1} are assigned to absorption bands related to stretching vibration of Fe–O in tetrahedral sites [33]. As and when the concentration of Sm, Nb are increased, the peak at 466 cm^{-1} shift towards higher frequency due to difference between the bond lengths of Fe–O and Nb–O, Sm–O and this small shift is minute. These bending vibrations along the polar axis indicate that the BTLF composites are purely tetragonal due to Ti–O stretching vibration along the polar axis of spontaneous polarization in BT with tetragonal phase [34] and no effective changes have been observed as and when doping with LF and Sm, Nb in BT.

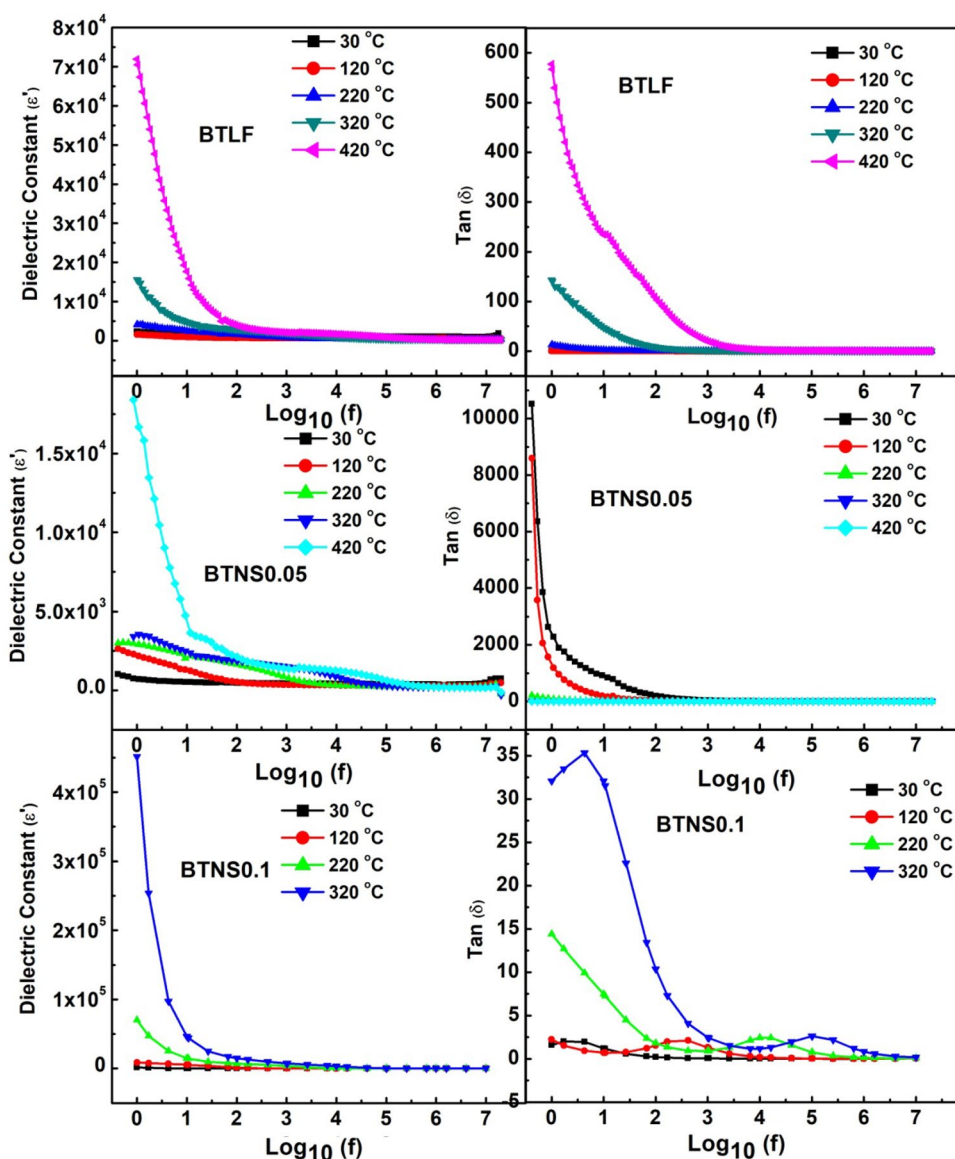
3.3 Dielectric studies

3.3.1 Variation of the dielectric constant and dielectric loss with frequency

The dielectric constant (ϵ') of BTLF, BTNS0.05 and BTNS0.1 composite with frequency at different temperatures (30 $^{\circ}\text{C}$, 120 $^{\circ}\text{C}$, 220 $^{\circ}\text{C}$, 320 $^{\circ}\text{C}$ and 420 $^{\circ}\text{C}$) are shown in Fig. 3. From Fig. 3 we clearly see that at 420 $^{\circ}\text{C}$, the dielectric constant (ϵ') of BTLF is high at low frequency region. The dielectric constant (ϵ') of BTLF decreases with an increase in the frequency till 100 Hz. Beyond the frequency 100 Hz, the dielectric constant (ϵ') becomes constant at all temperatures even after frequency is varied. At low frequency region, the dielectric constant (ϵ') of BTLF decreases when the temperature is decreased. The nature of dielectric constant (ϵ') of BTLF is same at all temperatures. Similar nature is also exhibited by BTLF when Sm and Nb are doped in it.

The value of dielectric constant of BTNS0.05 is less than BTLF and the dielectric constant of BTNS0.05 follow same trend as BTLF. We see from Fig. 3 that the dielectric constant of BTNS0.05 is high in low frequency region at high temperature and decreases steeply with increase in

Fig. 3 Variation of dielectric constant (ϵ') and dielectric loss ($\tan \delta$) of BTLF, BTNS0.05 and BTNS0.1 composite ceramics with frequency



frequency region at all temperatures up to frequency region between 35–0.16 MHz, beyond this frequency the dielectric constant becomes constant with increase in frequency at all temperatures.

The dielectric constant of BTNS0.1 is higher than BTLF, BTNS0.05 and the dielectric constant trend follow same as BTLF and BTNS0.05. The dielectric constant of BTNS0.1 is high in low frequency region at high temperature and decreases steeply with increase in frequency at all temperatures upto frequency 10 kHz, beyond this frequency the dielectric constant becomes constant with increases in temperature. The dielectric constant of BTLF is decreases by doping with Nb and Sm in BTLF and the dielectric constant of BTNS0.1 is higher than BTLF, BTNS0.05 which might be due to further increase in concentration of Nb, Sm in BTLF.

The dielectric constant of all composites is higher at low frequency regime due to interfacial polarization [35]. The dielectric constant of BTNS0.1 is higher than BTLF and BTNS0.05 which shows dispersion at lower frequency region can be explained by Maxwell Wagner interfacial polarization according to Koop's Theory [36, 37]. The dielectric constant reveals large values at low frequency regime for all composites due to reduction of space charge polarization caused by the heterogeneity in the composites [38]. At low frequency, the increase in the dielectric constant of all the composites with an increase in the temperature is due to the space charge polarization at the grain boundaries which creates a potential barrier. Because of this potential barrier, the charges are accumulated at the grain boundary which leads to high dielectric constant [39].

The dielectric loss ($\tan \delta$) of BTLF, BTNS0.05 and BTNS0.1 composites with frequency at different temperatures (30 °C, 120 °C, 220 °C, 320 °C and 420 °C) are shown in Fig. 3. We see from Fig. 3, that the nature of the dielectric loss of all composites is same as that of the dielectric constant (i.e.) the dielectric loss is high at low frequency and steeply decreases with an increase in the frequency till a certain frequency, beyond this frequency the dielectric loss attains nearly constant with further increase in the frequency. In low frequency regime, the dielectric loss of composites increases with increase in the temperature. From Fig. 3, we clearly see that the dielectric loss of BTLF increases when Nb and Sm are doped in it. Further when the concentration of Nb and Sm is increased from 0.05 to 0.10 the dielectric loss ($\tan \delta$) decreases. The dielectric loss of BTNS0.1 is lower than BTLF, BTNS0.05.

The high value of the dielectric loss of composites at low frequency region could be ascribed to the high resistivity at grain boundaries which are more effective than at grains [8].

3.3.2 Impedance (Z') varies with frequency

The frequency dependance of Impedance (Z') of BTLF, BTNS0.05 and BTNS0.1 composite ceramics at 30 °C, 120 °C, 220 °C, 320 °C and 420 °C are shown in Fig. 4. We see from Fig. 4c, that at low temperature, the impedance of all composites is high at low frequency region and decreases steeply with an increase in the frequency till a certain frequency and beyond this frequency, the impedance reaches nearly constant value with further increase in the frequency at all temperatures. At low frequency, the impedance of all composites exhibits dispersion with varying temperature. The impedance of BTLF, BTNS0.05 and BTNS0.1 decreases abruptly with an increase in the frequency till 50 Hz, 55 Hz and 100 kHz at low temperature. The decrease in the impedance (Z') of all composites with increase in the frequency and temperature clearly confirms that the conductivity is increasing with an increase in the frequency and temperature [4]. This rise in conduction with temperature may be due to the contribution of defects similar to oxygen vacancies. The impedance of all composites attain constant at all temperatures in high frequency region and this attainment of constant value represents a possibility of liberation of space charge as a consequence of lowering in the height of the barrier in the composite materials. Hence the electrical conduction will increase with an increase in the temperature [4].

3.3.3 Variation of dielectric constant (ϵ') with high frequency

The frequency dependance of dielectric constant (ϵ') of BTLF, BTNS0.05 and BTNS0.1 composite ceramics at 30 °C are

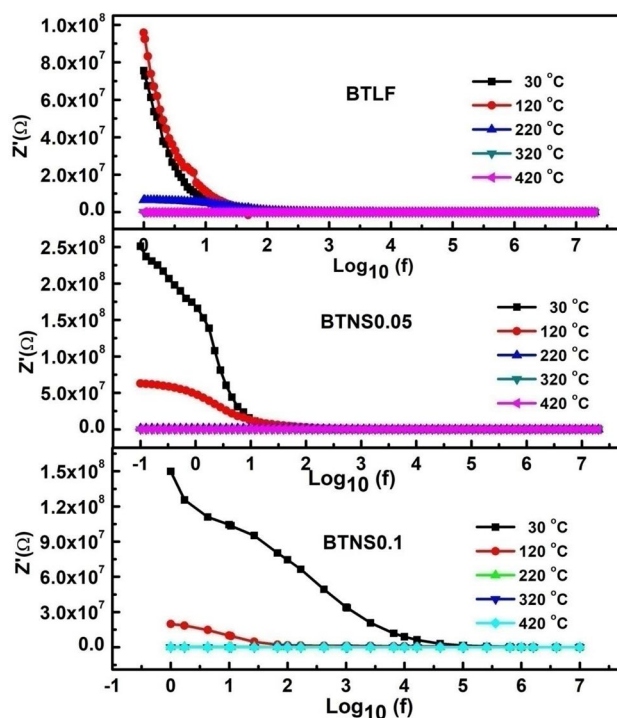


Fig. 4 Variation of impedance (Z') of BTLF, BTNS0.05 and BTNS0.1 composite ceramics with frequency

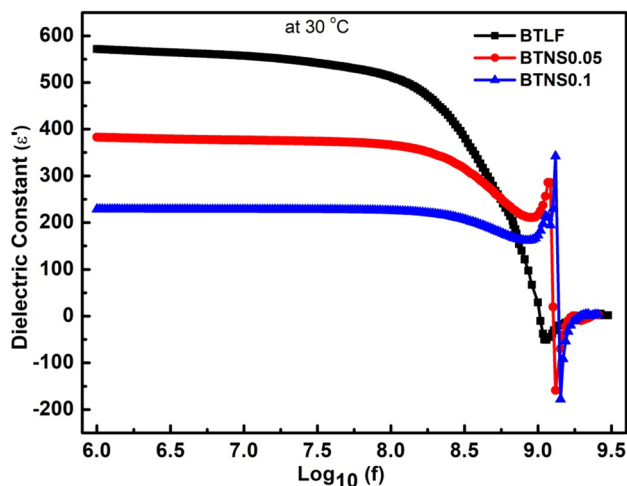


Fig. 5 Dielectric constant (ϵ') of BTLF, BTNS0.05 and BTNS0.1 composite ceramics varies with frequency (1 MHz–3.2 GHz) at 30 °C

shown in Fig. 5. Figure 5 clearly shows that the dielectric constant (ϵ') of BTLF, BTNS0.05 and BTNS0.1 composite decreases slightly and becomes constant with increase in the frequency from 1 MHz to 0.18 GHz, 1 MHz to 0.26 GHz and 1 MHz to 0.34 GHz respectively. Beyond these frequencies the dielectric constant of BTLF, BTNS0.05 and BTNS0.1 composite decreases rapidly with increase in the frequency till 1 GHz, 0.89 GHz and 0.97 GHz respectively.

Beyond these frequencies, the dielectric constant of BTLF, BTNS0.05 and BTNS0.1 composites shows complex behaviour. The complex behaviour in the dielectric constant of all samples has been already reported [39].

The dielectric constant (ϵ') of BTLF decreases after doping with Nb and Sm in BTLF and further decreases with an increase in the concentration of Nb and Sm in BTLF in the frequency region 1 MHz–1 GHz. We see from Fig. 5, the BTLF and Nb, Sm doped BTLF composites shows dispersion in the frequency region 1 MHz–0.56 GHz. The dielectric constant of composites attains nearly constant (dielectric relaxation) upto 0.34 GHz due to space charge polarization [40]. The dispersion occurring in the samples at higher frequencies suggests the inability of electrons to adapt to the applied field. The reason for the electrons not adapting to the applied field is due to the creation of uncompensated charges at the grain boundaries. The increase in the dielectric constant of all composites over the frequency range 1 MHz–1 GHz might be due to an increase in its grain size. The variation in the grain size or any other micro structural parameters induces relaxation effects in ferroelectric solid solution [41]. The rapid decrease in the dielectric constant of all composites lagging beyond 200 MHz shows its behaviour behind the frequency of the applied field at higher frequencies [42].

The high value of dielectric constant at lower frequency region is due to the presence of majority of elements like Fe^{2+} ions, oxygen vacancies and grain boundary defects [43]. Beyond the 1 GHz, the peaks show complex behaviour in all composites. The complex behaviour of the dielectric constant of all composites at high frequency region can be explained using Debye-type relaxation. According to Debye-type relaxation, the complex behaviour of dielectric constant arises when the jumping frequency of the Fe^{+2} and Fe^{+3} ions is exactly equal to the frequency of the applied field [40]. This type behaviour of dielectric constant at high frequency region might be used in high frequency microwave devices.

3.3.4 Variation dielectric loss ($\tan \delta$) with high frequency

The variation of dielectric loss ($\tan \delta$) of BTLF, BTNS0.05 and BTNS0.1 composite ceramics with frequency (1 MHz–3.2 GHz) at 30 °C are shown in Fig. 6. We see from Fig. 6, that the dielectric loss ($\tan \delta$) of BTLF, BTNS0.05 and BTNS0.1 composites attains almost constant with increase in frequency from 1 MHz to 100 MHz, 1 MHz to 0.20 GHz and 1 MHz to 1 GHz respectively. Beyond the frequencies 100 MHz, 0.20 GHz and 1 GHz, the dielectric loss ($\tan \delta$) increases steeply for BTLF, BTNS0.05 and BTNS0.1 composites respectively. The dielectric loss ($\tan \delta$) of BTLF initially decreases after substituting Nb and Sm in BTLF and again decreases with an

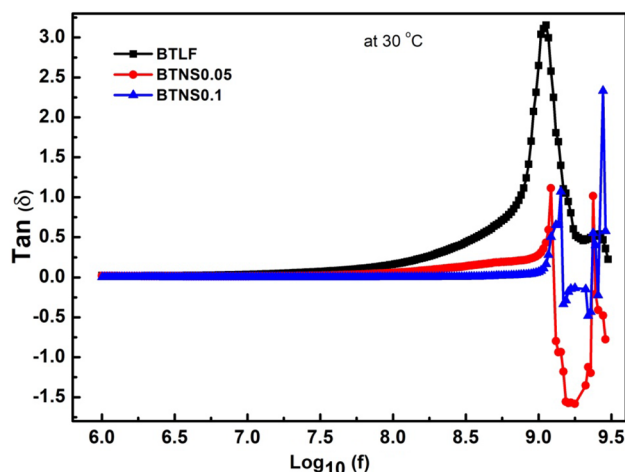


Fig. 6 Dielectric loss ($\tan \delta$) of BTLF, BTNS0.05 and BTNS0.1 composite ceramics varies with frequency (1 MHz–3.2 GHz) at 30 °C

increase in the concentration of Nb and Sm in BTLF in the frequency region 80 MHz–1.10 GHz. Beyond 1.10 GHz, the dielectric loss ($\tan \delta$) of all the composites exhibits jumping nature depicting complex behaviour.

The dielectric loss ($\tan \delta$) of all the composites attain constant upto 100 MHz frequency might be due to high resistivity at low frequency region. The high resistivity is due to the grain boundary effect which is pronounced more at low frequency region and hence more energy is dissipated for electron exchange between Fe^{2+} and Fe^{3+} ions, Sm^{+2} and Sm^{+3} ions or Nb^{+4} and Nb^{+5} . The resistivity is low due to grains which are more effective at high frequency region in which a small energy is required for exchange of electron between the two ferrite ions at the octahedral site [9]. Moreover the dielectric loss also depends on a number of components like stoichiometry ratio, structural homogeneity, number of Fe^{2+} ions which in turn is based on the composition and sintering temperature of the samples [44, 45]. Beyond the 1.10 GHz, the dielectric loss shows complex behaviour in all composites and this complex behaviour of the dielectric constant could be explained by Debye-type relaxation. According to Debye-type relaxation, the complex behaviour occurs when the jumping frequency of the Fe^{+2} and Fe^{+3} ions, Ti^{+3} and Ti^{+4} ions, Sm^{+2} and Sm^{+3} ions or Nb^{+4} and Nb^{+5} ions is exactly equal to the frequency of the applied field, i.e. $\omega\tau = 1$, where τ is the relaxation time of hopping process and ω is the angular frequency of the field. Thus as the Sm and Nb in composites increase, the energy loss decreases at high frequencies. At higher frequencies, the dielectric loss of materials is low presents the potential applications in high frequency microwave devices [46]. The value of dielectric loss ($\tan \delta$) of BTLF composites was found to be decreased from 3 to 0.135 in higher frequency region,

these materials having the potential applications in high frequency microwave devices [47].

3.4 Variation of A.C. conductivity with high frequency

The variation of conductivity of BTLF, BTNS0.05 and BTNS0.1 composite ceramics over the frequency region 1 MHz–3.2 GHz at 30 °C are shown in Fig. 7. From Fig. 7 we clearly see that the conductivity of BTLF increases with an increase in the frequency upto 0.1 GHz and beyond 0.1 GHz, the conductivity decreases with further increase in the frequency. The conductivity of BTLF exhibits a broad peak between the frequency 0.1 GHz and 0.87 GHz. The conductivity of BTLF initially increases after doping with Nb and Sm and further increases with an increase in the concentration of Nb and Sm. The conductivity of all composites shows dispersion characteristics between the samples. The conductivity peaks seen in Fig. 7 have shifted towards low frequency region. The reason for the shift of the conductivity peaks might be due to the substitution of Nb and Sm in BTLF and vacancies are formed along with depletion of Ti^{+4} and Ti^{+3} , Nb^{+5} and Nb^{+4} , Sm^{+3} and Sm^{+2} which may result in an electron conduction in order to maintain charge neutrality [24, 48]. The electrical conductivity is due to transition of electrons between ions of the same element present in more than one valence state. The nature of conductivity of BTNS0.05 is same as the conductivity of BTLF. The conductivity BTNS0.05 is higher than that of BTLF and exhibits broad peak at 0.85 GHz. The conductivity of BTNS0.1 increases steeply with an increase in the frequency till 0.298 GHz, beyond this frequency, the conductivity decreases with further increase in the frequency till 1.7 GHz. The conductivity of BTNS0.1 exhibits a sharp

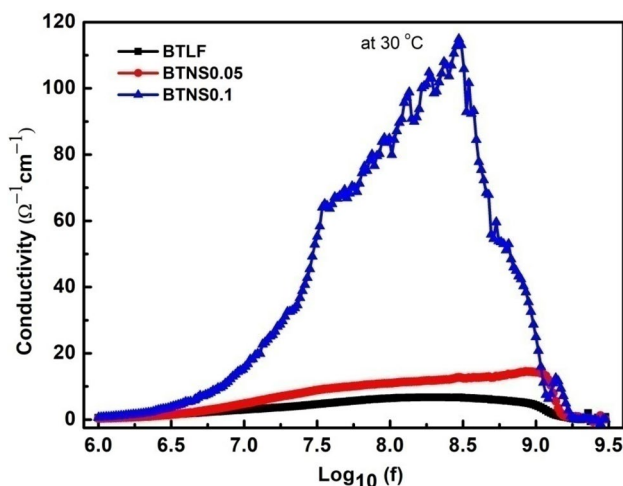


Fig. 7 Conductivity of BTLF, BTNS0.05 and BTNS0.1 composite ceramics varies with frequency (1 MHz–3.2 GHz) at 30 °C

peak at 0.298 GHz which represents the phase change. The conductivity of all the composites reaches constant value beyond 1.7 GHz. The increase in the conductivity of BTLF composite with the frequency may be due to hopping of electrons between ions. The conductive grains become vigorous by inducing the hopping between ions when the frequency is increased. The electrons start hopping between ions at which frequency is consider as hopping frequency [9]. As the frequency of the applied field increases, the hopping frequency also increases and hence the conductivity increases gradually with frequency [49]. Beyond the frequency 1.7 GHz, the BTLF shows relaxation species. This may be due to the hopping of electrons at high frequency region.

3.5 Variation of Impedance (Z') with high frequency

The variation of impedance (Z') of BTLF, BTNS0.05 and BTNS0.1 composite ceramics over the frequency region 1 MHz–3.2 GHz at 30 °C are shown in Fig. 8. The impedance (Z') of all composites decreases with an increase in the frequency till 32 MHz, beyond this frequency, the impedance (Z') of all composites become frequency independent till 1 GHz which is clearly shown in the inset of Fig. 8. Beyond the frequency 1 GHz, the impedance (Z') of all composites shows a complex behaviour. The impedance of the composites depicts a complex behaviour which is due to an increase in the AC conductivity. The enhancement in the A.C. conductivity material indicates the presence of relaxation species and also non Debye type of relaxation process takes place in the composite materials [50, 51]. We see from Fig. 8, at low frequency region, the impedance (Z') of BTLF decrease slightly after doping Nb and Sm in BTLF

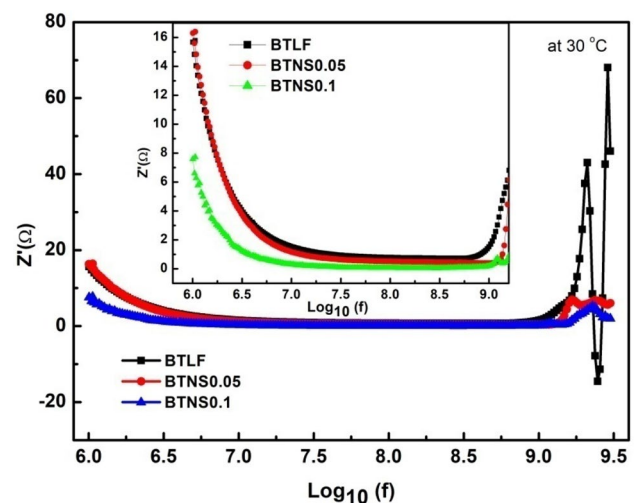
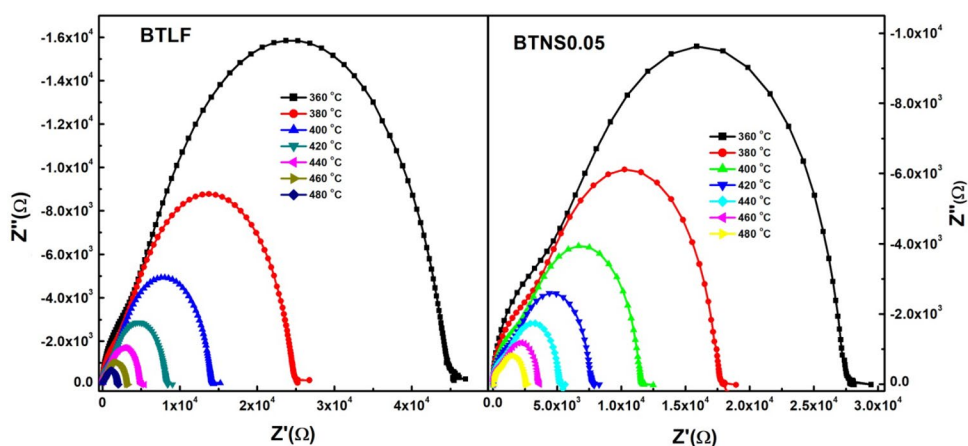


Fig. 8 Variation of impedance (Z') for BTLF, BTNS0.05 and BTNS0.1 composite ceramics with high frequency (1 MHz–3.2 GHz) at 30 °C. Inset shows impedance (Z') with frequency region between 1 MHz–3 GHz

Fig. 9 Variation of impedance (Z') with complex impedance (Z'') of BTLF and BTNS0.05 composite ceramics



and further decrease with increase in concentration of Nb and Sm in BTLF. The impedance (Z') of composites indicates the presence of dispersion at lower frequency region which might be due to the substitution of Nb and Sm in BTLF. The impedance (Z') of BTLF composites decreases with an increase in the frequency and the impedance of all the composites becomes constant in the high frequency region 32 MHz–1 GHz. The reason for the impedance of all the composites becoming independent of the frequency may be because of an increase in the ac conductivity due to release of space charge as a consequence of reduction in barrier height [52].

3.6 Nyquist plots

The variation of impedance (Z') with complex impedance (Z'') spectra (Nyquist plots) of BTLF and BTNS0.05 composites at different temperatures over the frequency region 1 Hz–10 MHz are shown in Fig. 9. We see from Fig. 9 that the impedance spectrum exhibits good semi circles with their centres situated at real axis (Z') and all the semi circles are completed at all temperatures. The radius of all semi-circles decreases with an increase in the temperature. The decrease in the radius of all semi-circles is due to the increase in the conductivity of all composites with increase in the temperature [53]. We see from Fig. 9, that the area under the semicircles of BTNS0.05 is smaller than BTLF due to Nb, Sm doped in BTLF. At all temperatures, the entire semi circles of BTLF and BTNS0.05 composites forming their centers at real axis (Z') can be explained by Debye's model. Debye's model describes that the reason for the appearance of a semicircle having centre on the real axis is due to a single relaxation time of a material. The formation of impedance plots seems to be a cole-cole plot which suggests that the electrical response is made up of more than two relaxation phenomena with different relaxation frequencies. The impedance of semicircles at high frequency is caused by the bulk property of the materials and impedance

arc of semicircles at low frequency is ascribed to the grain boundary in the materials [4].

4 Conclusions

The Sm and Nb doped $\text{BaTiO}_3\text{-Li}_{0.5}\text{Fe}_{2.5}\text{O}_4$ composite ceramics were successfully synthesized by solid state reaction technique. The X-Ray diffraction peaks of BTNS0.05 and BTNS0.1 have shifted towards higher diffraction angle which confirms the incorporation Nb and Sm in BTLF. The bending vibrations along the polar axis suggest existence of a pure tetragonal phase. The dielectric constant of BTNS0.1 is higher than BTLF, BTNS0.05 which shows dispersion at low frequency region. The dielectric constant of composites attains nearly constant (dielectric relaxation) up to 0.34 GHz. The impedance value attainment of constants of all composites at all temperatures in high frequency region suggests the possibility of the release of space charge. The dielectric constant of BTLF, BTNS0.05 and BTNS0.1 composites show jumping behaviour beyond 1 GHz. The decrease in the dielectric loss of BTLF at high frequency region is due to the substitution of Nb and Sm in BTLF. The conductivity of composites has increased after incorporation of Nb and Sm in BTLF composites and the conductivity peaks have shifted towards the low frequency region. The impedance (Z') of all composites decreases with an increase in the frequency till 32 MHz. At all temperatures, the impedance spectrum of BTLF and BTNS0.05 composites exhibits complete semi circles with their centers situated at the real axis (Z'). These properties confirm the applications of the BTLF material in high frequency microwave devices.

Acknowledgements We would like to thank Dr. P.D Babu of UGC-DAE Consortium for Scientific Research, Mumbai center, R5-shed, BARC, Mumbai—400 085 for extending the facilities and his support. We would also like to thank Dr. V. Raghavendra Reddy and Dr. Mukul Gupta of UGC-DAE Consortium for Scientific Research, Indore for

extending the facilities and their support. We also thank INUP, IITB for extending the facilities Dielectric measurements.

References

- P.K. Patel, J. Rani, N. Adhlakha, H. Singh, K.L. Yadav, Enhanced dielectric properties of doped barium titanate ceramics. *J. Phys. Chem. Solids* **74**, 545–549 (2013)
- H. Haibo Yang, L. Wang, X. He, Yao, Hexagonal BaTiO₃/Ni_{0.8}Zn_{0.2}Fe₂O₄ composites with giant dielectric constant and high permeability. *Mater. Chem. Phys.* **134**, 777–782 (2012)
- T. Xu, L. Chen, Z. Guo, T. Ma, Strategic improvement of the long-term stability of perovskite materials and perovskite solar cells. *Phys. Chem. Chem. Phys.* **18**, 27026–27050 (2016)
- T. Badapanda, S. Sarangi, S. Parida, B. Behera, B. Ojha, S. Anwar, Frequency and temperature dependence dielectric study of strontium modified Barium Zirconium Titanate ceramics obtained by mechanochemical synthesis. *J. Mater. Sci.: Mater. Electron.* **26**(5), 3069–3082 (2015)
- B. Luo, X. Wang, E. Tian, G. Li, L. Li, Electronic structure, optical and dielectric properties of BaTiO₃/CaTiO₃/SrTiO₃ ferroelectric super lattices from first principles calculations. *J. Mater. Chem. C* **3**, 8625–8633 (2015)
- J.F. Scott, *Appl. Mod. Ferroelectr. Sci.* **315**, 954–959 (2007)
- X. Na Zhu, X. Chen, H. Tian, X.M. Chen, Atomic scale investigation of enhanced ferroelectricity in (Ba, Ca) TiO₃. *RSC Adv.* **7**, 22587–22591 (2017)
- Ch Rayssi, S. El.Kossi, J. Dhahri, K. Khirouni, Frequency and temperature-dependence of dielectric permittivity and electric modulus studies of the solid solution Ca_{0.85}Er_{0.1}Ti_{1-x}Co_{4x/3}O₃ (0 ≤ x ≤ 0.1) *RSC Adv.* **8**, 17139–17150 (2018)
- S.B. Narang, D. Kaur, K. Pubby, Frequency and temperature dependence of dielectric and electric properties of Ba_{2-x}Sm_{4+2x/3}Ti₈O₂₄ with structural analysis. *Mater. Sci. –Pol.* **33**(2), 268–277 (2015)
- N.P. Chermisinoff (ed.), *Handbook of Ceramics and Composites, Synthesis and Properties*, (Marcel Dekker Inc., New York, 1990)
- W. Cai, C. Fu, J. Gao, X. Deng, G. Chen & Z. Lin, Effect of samarium on the microstructure, dielectric and ferroelectric properties of barium titanate ceramics. *Integr. Ferroelectr.* **140**, 92–103 (2012)
- W. Cai, C.L. Fu, J.C. Gao et al., Dielectric properties and microstructure of Mg doped barium titanate ceramics. *Adv. Appl. Ceram.* **110**(3), 181–185 (2011)
- A.K. Nath, N. Medhi, Piezoelectric properties of environmental friendly bismuth doped barium titanate ceramics. *Mater. Lett.* **73**, 75–77 (2012)
- Y.X. Li, X. Yao, X.S. Wang et al., Studies of dielectric properties of rare earth (Dy, Tb, Eu) doped barium titanate sintered in pure nitrogen. *Ceram. Int.* **38**(S1), S29–S32 (2011)
- V.V. Mitic, Z.S. Nikolic, V.B. Pavlovic et al., Influence of rare-earth dopants on barium titanate ceramics microstructure and corresponding electrical properties. *J. Am. Ceram. Soc.* **93**(1), 132–137 (2010)
- Y. Yuan, S.R. Zhang, X.H. Zhou, B. Tang, Effects of Nb₂O₅ doping on the microstructure and the dielectric temperature characteristics of barium titanate. *J. Mater. Sci.* **44**(14), 3751–3757 (2009)
- M.M. Vijatović Petrović, J.D. Bobić, T. Ramoška et al., Antimony doping effect on barium titanate structure and electrical properties. *Ceram. Int.* **37**(7), 2669–2677 (2011)
- M.C. Ferrarelli, C.C. Tan, D.C. Sinclair, Ferroelectric, electrical, and structural properties of Dy and Sc co-doped BaTiO₃. *J. Mater. Chem.* **21**(17), 6292–6299 (2011)
- Y.-P. Fua, D.-S. Hung, Y.-D. Yao, Microwave properties of chromium-substituted lithium ferrite. *Ceram. Int.* **35**(6), 2179–2184 (2009)
- A. Verma, T.C. Goyal, R.G. Mindiretta, R.G. Gupta, High-resistivity nickel–zinc ferrites by the citrate precursor method. *J. Magn. Magn. Mater.* **192**(2), 271–276 (1999)
- M.A. El Hiti, Dielectric behavior and ac electrical conductivity of Zn-substituted Ni-Mg ferrites. *J. Magn. Magn. Mater.* **164**(1–2), 187–196 (1996)
- Seema Verma, P.A. Joy, Magnetic properties of super paramagnetic lithium ferrite nanoparticles. *J. Appl. Phys.* **98**(12), 124312–124319 (2005)
- S.B. Narang, S. Bahel, Low loss dielectric ceramics for microwave applications: a review. *J. Ceram. Process. Res.* **11**(3), 316–321 (2010)
- S. B. Narang, D. Kaur, K. Pubby, Effect of Substitution of Samarium and Lanthanum on Dielectric and Electrical Properties of Barium Titanate. *Ferroelectrics* **486**, 74–85 (2015)
- J. Li, H. Kakemoto, S. Wada, T. Tsurumi, Dielectric properties of BaTiO₃-based ceramics measured up to GHz region. *J. Electroceram.* **21**, 427–430 (2008)
- P. Padmini, T.R. Taylor, M.J. Lefevre, A.S. Nagre, R.A. York, J.S. Speck, Realization of high tunability barium strontium titanate thin films by rf magnetron sputtering. *Appl. Phys. Lett.* **75**, 3186–3188 (1999)
- Y. Gim, T. Hudson, Y. Fan, C. Kwon, T. Findikoglu, B.J. Gibbons, B.H. Park, Q.X. Jia, Microstructure and dielectric properties of Ba_{1-x}Sr_xTiO₃Ba_{1-x}Sr_xTiO₃ films grown on LaAlO₃ substrates. *Appl. Phys. Lett.* **77**, 1200–1202 (2000)
- J. Im, O. Auciello, P.K. Baumann, S.K. Streiffer, D.Y. Kaufman, A.R. Krauss, Composition-control of magnetron-sputter-deposited (Ba_xSr_{1-x})Ti_{1+y}O_{3+z} thin films for voltage tunable devices. *Appl. Phys. Lett.* **76**, 625–627 (2000)
- G.RaoG.L.R. Buddiga, K.N. Chidambara Kumar, M. Dasari, Influence of Sm and Nb on the structural, electric, magnetic and magneto-electric properties of BaTiO₃-Li_{0.5}Fe_{2.5}O₄ composite ceramics grown by the conventional solid state technique. *J. Mater. Sci.: Mater. Electron.* (2018). <https://doi.org/10.1007/s10854-018-0394-1>
- C.M.B. Henderson, J.M. Charnock, G. Cressey, D.T. Griffen, An EXAFS study of the local structural environments of Fe, Co, Zn and Mg in natural and synthetic staurolites. *Miner. Mag.* **61**, (408) 613–625 (1997)
- D.M. Sherman, The electronic structures of manganese oxide minerals. *Am. Mineral.* **69**, 788–799 (1984)
- A.B. Gadkari, T.J. Shinde, P.N. Vasambekar, Structural analysis of Y³⁺-doped Mg–Cd ferrites prepared by oxalate co-precipitation method. *Mater. Chem. Phys.* **114**, 505–510 (2009)
- N.M. Deraz, Fabrication, characterization and magnetic behaviour of alumina-doped zinc ferrite nano-particles. *J. Anal. Appl. Pyrol.* **91**(1), 48–54 (2011)
- A. Abdel Aal, T.R. Hammad, M. Zawrah, I.K. Battisha, A.B. Abou Hammad, FTIR Study of Nanostructure Perovskite BaTiO₃ Doped with Both Fe³⁺ and Ni²⁺ Ions Prepared by Sol-Gel Technique, *Acta Phys. Pol. A*, 126 (6) (2014) 1318–1322
- N. Ashutosh Mishra, S. Mishra, K.M. Bisen, Jarabana, Frequency and temperature dependent dielectric studies of BaTi_{0.96}Fe_{0.04}O₃. *International Conference on Recent Trends in Physics (ICRTP 2014)*
- R. Sharma, V. Singh, R.K. Kotnala, R.P. Tandon, Investigation on the effect of ferrite content on the multiferroic properties of (1-x) Ba_{0.95}Sr_{0.05}TiO₃ - (x) Ni_{0.7}Zn_{0.2}Co_{0.1}Fe₂O₄ ceramic composite. *Mater. Chem. Phys.* **160**, 447–455 (2015)
- C.G. Koops, On the dispersion of resistivity and dielectric constant of some semiconductors at audio frequencies. *Phys. Rev.* **83**, 121–124 (1951)

38. S.N. Babu, J.-H. Hsu, Y.S. Chen, J.G. Lin, Magnetoelectric response in lead-free multiferroic $\text{NiFe}_2\text{O}_4\text{-Na}_{0.5}\text{Bi}_{0.5}\text{TiO}_3$ composites, *J. Appl. Phys.* **109**, 07D904 1–07D904 34 (2011)
39. M. Asif Iqbal, M.U. Islama, I. Ali, M. Azhar khan, I. Sadiq, I. Ali, High frequency dielectric properties of Eu^{+3} -substituted Li–Mg ferrites synthesized by sol–gel auto-combustion method. *J. Alloys Compd.* **586**, 404–410 (2014)
40. N. Rezlescu, E. Rezlescu, Dielectric Properties of Copper Containing Ferrites. *Phys. Status Solidi A.* **23**, 575–582 (1974)
41. C.E. Ciomaga, R. Calderone, M.T. Buscaglia, M. Viviani, V. Buscaglia, L. Mitoseriu, A. Stancu, P. Nanni, Relaxor properties of $\text{Ba}(\text{Zr,Ti})\text{O}_3$ ceramics. *J. Optoelectron. Adv. Mater.* **8**(3), 944–948 (2006)
42. B. Chandra Babu, V. Naresh, B. Jayaprakash, S. Buddhudu, Structural, thermal and dielectric properties of lithium zinc silicate ceramic powders by sol-gel method. *Ferroelectr. Lett.* **38**, 114–127 (2011)
43. B. Baruwati, K.M. Reddy, V. Sunkara, R.K. Manorama, O. Singh, J. Prakash, Tailored conductivity behavior in nanocrystalline nickel ferrite. *Appl. Phys. Lett.* **85**(14), 2833–2835 (2004)
44. R.G. Kharabe, R.S. Devan, C.M. Kanamadi, B.K. Chougale, Dielectric properties of mixed Li-Ni-Cd ferrites. *Smart Mater Struct* **15**, 36–39 (2006)
45. R.S. Devan, B.K. Chougale, Effect of Composition on coupled electric magnetic and dielectric properties of two phase particulate magnetoelectric composite. *J. Appl. Phys.* **101**(1), 014109–014106 (2007)
46. M.T. Farid, I. Ahmad, S. Aman, M. Kanwal, G. Murtaza, I. Ali, I. Ahmad, M. Ishfaq, Structural, electrical and dielectric behavior of $\text{Ni}_x\text{Co}_{1-x}\text{Pr}_y\text{Fe}_{2-y}\text{O}_4$ nano-ferrites synthesized by sol-gel method. *Dig. J. Nanomater. Biostruct.* **10**(1), 265–275 (2015)
47. M. Raghasudha, D. Ravinder, P. Veera somaiah, Influence of Cr^{3+} ion on the dielectric properties of nano crystalline Mg-ferrites synthesized by citrate-gel method. *Mater. Sci. Appl.* **4**(7), 432–438 (2013)
48. S.B. Narang, D. Kaur, K. Pubby, Dielectric and impedance spectroscopy of samarium and lanthanum doped barium titanate at room temperature. *Int. Sch. Sci. Res. Innov.* **9**(6), 667–671 (2015)
49. N. Zidi, A. Chaouchi, S. d’Astorg, M. Rguiti, C. Courtois, Dielectric and impedance spectroscopy characterizations of CuO added $(\text{Na}_{0.5}\text{Bi}_{0.5})_{0.94}\text{Ba}_{0.06}\text{TiO}_3$ lead-free piezoelectric ceramics. *J. Alloys Compd.* **590**, 557–564 (2014)
50. R.-H. Yue-MingLi, X.-P. Liao, Y.-P. Jiang, Zhang, Impedance spectroscopy and dielectric properties of $\text{Na}_{0.5}\text{Bi}_{0.5}\text{TiO}_3\text{-K}_{0.5}\text{Bi}_{0.5}\text{TiO}_3$ ceramics. *J. Alloys Compd.* **484**, 961–965 (2009)
51. K.C. Verma, S.K. Tripathi, R.K. Kotnala, Surface spins enhanced magnetoelectric coefficient and impedance spectroscopy of $\text{BaFe}_{0.01}\text{Ti}_{0.99}\text{O}_3$ and $\text{BaFe}_{0.015}\text{Ti}_{0.985}\text{O}_3$ nanorods. *Mater. Res. Bull.* **68**, 331–335 (2015)
52. K.C. Verma, M. Ram, J. Singh, R.K. Kotnala, Impedance spectroscopy and dielectric properties of Ce and La substituted $\text{Pb}_{0.7}\text{Sr}_{0.3}(\text{Fe}_{0.012}\text{Ti}_{0.988})\text{O}_3$ nanoparticles. *J. Alloys Compd.* **509**, 4967–4971 (2011)
53. R. Poonam Kumari, S. Rai, Sharma†, M.A. Valente, Dielectric, electrical conduction and magnetic properties of multiferroic $\text{Bi}_{0.8}\text{Tb}_{0.1}\text{Ba}_{0.1}\text{Fe}_{0.9}\text{Ti}_{0.1}\text{O}_3$ perovskite compound. *J. Adv. Dielectr.* **7**(5), 1750034 (2017)